

Ultrathin Film Electrodeposition of Polythiophene Conjugated Networks through a Polymer Precursor Route

Chuanjun Xia, Xiaowu Fan, Mi-kyoung Park, and Rigoberto C. Advincula*

Department of Chemistry, University of Alabama at Birmingham,
Birmingham, Alabama 35294-1240

Received August 9, 2001. In Final Form: October 3, 2001

The electrodeposition of polysiloxane precursor polymers to form cross-linked conjugated polythiophene ultrathin films is described. The precursor polymer contains a polysiloxane backbone with pendant electroactive thiophene monomer units synthesized via a hydrosilylation reaction. The thiophene units were electropolymerized by cyclic voltammetry. Investigations were made on the oxidation and reduction of the thiophene monomer and the polymers formed. A uniformly smooth layer-by-layer growth of the film was observed by repeated cycling based on the cyclic voltammogram, surface plasmon spectroscopy (SPS), and the atomic force microscopy images. The morphology of the film changed with increasing number of cycles being transformed from a relatively globular to a more membranelike morphology. Correlation was also made on the morphological changes with the electropolymerization process and the extent of cross-linking. UV–vis spectra showed clear evidence of polythiophene structure formation in the cross-linked polymer. SPS confirmed that the thickness of the deposited polymer film is easily controlled by the number of electrochemical potential cycles.

Introduction

Substituted polythiophenes are materials of great interest.¹ These π -conjugated organic polymers have been widely investigated in the past decade, both for fundamental reasons and because of their potential for device applications, for example, in the field of electronics and electro-optics. A number of methods have been developed to synthesize this class of materials, both chemically and electrochemically.² Electrochemical synthesis utilizes the ability of the monomer to be coupled upon oxidation.³ While it can cause structural defects on the polymer backbone, electropolymerization nonetheless is a rather convenient alternative since it avoids the need for polymer isolation and purification. Various polythiophene derivatives have been designed and made. They have found applications in polymer light emitting diode (PLED),⁴ field-effect transistor (FET) devices,⁵ electrochromic devices,⁶ and sensors.⁷ For thin film devices, high quality films of good optical and electronic properties are necessary for high performance. However, it is well-known that films electrodeposited on a conducting substrate directly from monomer units normally have rough surface morphologies.⁸ This is due to the rapid propagation step for the polymerization and precipitation of the polymer out of

the solution.⁹ For thin and ultrathin film electro-optical and optical applications involving these polymers, thicknesses on flat surfaces are in the order of a few to several hundred nanometers. Optimization is necessary to get homogeneous surface coverages and smooth morphologies.¹⁰

Recently, we have reported a novel method for depositing high optical quality ultrathin films of conjugated polymers on conducting substrates via electrochemistry and rational polymer design.¹¹ We have initially investigated this “precursor polymer” route by depositing and patterning films using electrochemical methods and applying them on the fabrication of PLED structures.¹² A polymer precursor, which contained pendant electroactive monomer units, was first synthesized by conventional chemical methods. The precursor was then electropolymerized and deposited on the conducting substrate. This method is generally applicable to a variety of systems with different polymer backbones and monomer units.¹³ Thus, it is possible to investigate different monomer and precursor polymer compositions, monomers, and mixed systems. The general principle for the precursor polymer approach is shown in Scheme 1.

In this paper, we describe our initial results on the electropolymerization, cross-linking, and ultrathin film deposition of polymethylsiloxane-modified polythiophene precursor polymers. Because of the potential for electro-

(1) (a) Roncali, J. *Chem. Rev.* **1992**, *92*, 711. (b) Chan, H.; Ng, S. *Prog. Polym. Sci.* **1998**, *23*, 1167. (c) Roncali, J. *Chem. Rev.* **1997**, *97*, 173.

(2) (a) McCullough, R. D.; Ewbank, P. C.; Loewe, R. S. *J. Am. Chem. Soc.* **1997**, *119*, 633. (b) Reddinger, J.; Reynolds, J. *Adv. Polym. Sci.* **1999**, *145*, 57.

(3) (a) Kuwabata, S.; Ito, S.; Yoneyama, H. *J. Electrochem. Soc.* **1988**, *135*, 1691. (b) Ingnas, O.; Liedberg, B.; Chang-Ru, W. *Synth. Met.* **1985**, *11*, 239.

(4) Kraft, A.; Grimsdale, A. C.; Holmes, A. B. *Angew. Chem., Int. Ed.* **1998**, *37*, 402.

(5) Bao, Z.; Feng, Y.; Dodabalapur, A.; Raju, V. R.; Lovinger, A. J. *Chem. Mater.* **1997**, *9*, 1299.

(6) (a) Sankaran, B.; Reynolds, J. *Macromolecules* **1997**, *30*, 2582. (b) Kumar, A.; Reynolds, J. *Macromolecules* **1996**, *29*, 7629. (c) Kumar, A.; Welsh, D.; Morvant, M.; Piroux, F.; Abboud, K.; Reynolds, J. *Chem. Mater.* **1998**, *10*, 896.

(7) McQuade, T.; Pullen, A.; Swager, T. *Chem. Rev.* **2000**, *100*, 2537.

(8) (a) Sayre, C.; Collard, D. *Langmuir* **1997**, *13*, 714. (b) Li, J.; Josowicz, M. *Chem. Mater.* **1997**, *9*, 1451.

(9) Berlin, A. *In Electrical and optical polymer systems – fundamentals, methods, and applications*; Wise, D. L., Wnek, G. E., Trantolo, D. J., Cooper, T. M., Gresser, J. D., Eds.; Marcel Dekker: New York, 1993; p 47.

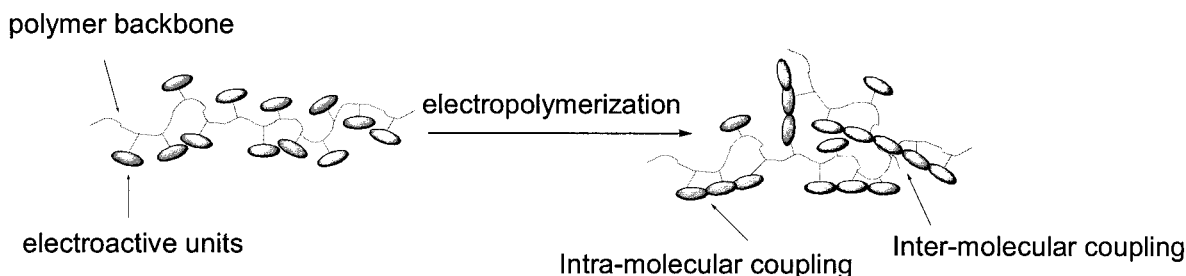
(10) Gonçalves, D.; Irene, E. *Langmuir* **2001**, *17*, 5031.

(11) Inaoka, S.; Roitman, D.; Advincula, R. *Polym. Prepr. (Am. Chem. Soc., Div. Polym. Chem.)* **2000**, *41* (1), 808. Advincula, R.; Inaoka, S.; Roitman, D. Full manuscript in preparation.

(12) Advincula, R.; Inaoka, S.; Roitman, D. Molecularly Ordered π -Conjugated Polymer Networks on Conducting Surfaces using the Precursor Polymer Approach: A New Approach for Solid-State Applications. *Proc. SPIE–Int. Soc. Opt. Eng.*, in press.

(13) Submitted chapter review: Advincula, R.; Xia, C.; Inaoka, S.; Roitman, D. Ultrathin Films of Conjugated Polymers on Conducting Surfaces. In *Thin Films*; Soriaga, M., Ed.; for release in 2001.

Scheme 1. Schematic Drawing of the Precursor Polymer Approach after Electropolymerization Resulting in Cross-Linked Network Structure



optical applications, we have used the unique properties of silicone polymers toward depositing ultrathin films of conjugated polymers with *high optical quality* on surfaces. The poly(dimethylsiloxane) backbone is a good starting point because of its low glass transition temperature or T_g , inertness, and low reactivity compared with other polyolefinic and methacrylate polymers.¹⁴

Experimental Section

Instrumentation. The NMR spectra were collected on a Bruker ARX 300 spectrometer with chloroform-*d* as solvent and tetramethylsilane as internal standard. UV-vis spectra were obtained on a Perkin-Elmer Lambda 20 spectrometer. Size-exclusion chromatography (SEC) data were measured on a Waters Chromatography setup using polystyrene as the standard. Cyclic voltammetry (CV) was performed on an Amel 2049 potentiostat and Power lab system with a three-electrode cell. Atomic force microscopy (AFM) imaging was performed in air using a PicoScan system (Molecular Imaging) equipped with an $8 \times 8 \mu\text{m}$ scanner. Magnetic-ac (Mac) mode (a noncontact mode) was used for all the AFM images. A Mac lever, a silicon-nitride-based cantilever coated with magnetic film, was used as an AFM tip. Surface plasmon spectroscopy (SPS) using a 632.8 nm He-Ne laser was measured using the Multiskop instrument (Optrel GmbH) on ultrathin films electrodeposited on an Au-coated (45 nm) BK-7 glass.²⁴ In general, SPS allows for the elucidation of thickness and refractive index (dielectric constants) using the attenuated total reflection (ATR). This is done by prism coupling of incident light at a thin Au surface in the presence of a dielectric film material. Together with a known refractive index (1.54), fitting using a Fresnel formula algorithm allows for the calculation of the optical thickness. X-ray photoelectron spectroscopy (XPS) on the electrodeposited films was done on a Kratos Axis 165 Multitechnique Electron Spectrometer system. A monochromatic Al K α X-ray source (1486.6 eV) was applied to excite the photoemission. Survey scans were collected from 0 to 1400 eV to obtain elemental composition information.

Synthesis. *Synthesis of 3-Undec-10-enyl-thiophene.*¹⁵ To a suspension of 1.46 g of magnesium in 20 mL of ether, 11.66 g of 11-bromo-1-undecene in 20 mL of ether was added dropwise. After reacting for 2 h, the formed Grignard reagent was transferred to another flask dropwise at 0 °C in which was charged 6.79 g of 3-bromothiophene, 0.20 g of Ni(dppp)Cl_2 , and 40 mL of ether. The mixture was allowed to warm to room temperature, stirred overnight, and then quenched with dilute hydrochloric acid, extracted with ether, and dried over magnesium sulfate. The crude product was purified by column chromatography using hexanes as eluent. Pure product (5.6 g) was obtained; yield, 57%. $^1\text{H NMR}$: δ (ppm) 7.23 (q, 1H), 6.94–6.88 (m, 2H), 5.82 (m, 1H), 4.94 (m, 2H), 2.62 (t, 2H), 2.00 (p, 2H), 1.65 (p, 2H), 1.39–1.21 (m, 14H). $^{13}\text{C NMR}$: δ (ppm) 143.68, 139.68, 128.72, 125.46, 120.18, 114.54, 34.26, 30.99, 30.71, 30.13, 29.96, 29.91, 29.88, 29.76, 29.57, 29.37.

*Synthesis of Poly(methyl-(10-thiophen-3-yl-decyl)siloxane).*¹⁶ In a one-neck flask, 0.53 g of polydihydrodimethylsiloxane (Aldrich), 2.36 g of 3-undec-10-enyl-thiophene, 0.02 g of H_2PtCl_6 , and 10 mL of methylene chloride were added under nitrogen. The mixture was sonicated and stopped until the NMR showed no Si-H proton signals. The resulting mixture was solvent evaporated and run through flash column chromatography using hexanes and ethyl acetate as eluent. Thiophene-modified polysiloxane (2.0 g) was obtained. $^1\text{H NMR}$: δ (ppm) 7.22 (b, 1H), 6.91 (b, 1H), 2.61 (b, 2H), 1.61 (b, 2H), 1.29 (b, 22H), 0.50 (b, 2H), 0.06 (m, 5H).

Electrodeposition of the Precursor Polymer. In a three-electrode cell, the solution contained poly(methyl-(10-thiophen-3-yl-decyl)siloxane), 0.1 M tetrabutylammonium hexafluorophosphate (TBAH), and methylene chloride. The polymerization was performed by sweeping the potential from -400 to 1500 mV versus the Ag/Ag^+ (0.01 M in acetonitrile) reference electrode. After the desired number of cycles, the substrate was maintained at the initial potential for 10 min and then taken out and rinsed with methylene chloride, acetone, and methanol thoroughly. The substrate was finally dried under dry nitrogen flow.

Results and Discussion

The synthetic scheme for the polymethylalkylthiophene-siloxane precursor polymer is shown in Scheme 2. The alkene-terminated thiophene was made through a Grignard coupling reaction. The reaction also gave a small amount of isomerized product that cannot undergo the hydrosilylation reaction, and it was easily separated during purification after the hydrosilylation step. The hydrosilylation reaction was performed using a platinum catalyst. The reaction was monitored by NMR and was complete in less than half an hour. The resulting polymer has a number-average molecular weight of 8000 g mol^{-1} as measured by SEC using a polystyrene standard.

The electrodeposition of the precursor polymer was performed on a conventional three-electrode cell design, which has a gold-coated BK7 glass working electrode, a gold-coated BK7 glass counter electrode, and an Ag/Ag^+ reference electrode. The electropolymerization was done by cyclic voltammetry with a scan rate of 100 mV/s . The CVs obtained from different concentrations of the polymer are shown in Figure 1. The anodic peak at ca. 0.62 V , corresponding to the oxidation of the polymeric thiophene, typically appeared in the second cycle.¹⁷ The peak potential shifted gradually toward higher values as the thickness of the films increased. This potential shift is attributed to heterogeneous electron-transfer kinetics, IR drop of the film ($V_{\text{total}} = V_{\text{across film}} + I(R_{\text{film}} + R_{\text{soln}})$), and a decrease of the film conductivity.¹⁸ However, as the concentration of the precursor polymer decreased, this potential shift

(14) (a) Clarson, S.; Fitzgerald, J.; Smith, S.; Owen, M. *Silicones and Silicone-Modified Materials*; American Chemical Society: Washington, DC (distributed by Oxford University Press), 2000. (b) *The Chemistry of Organic Silicon Compounds*; Patai, S., Rappoport, Z., Eds.; Wiley: Chichester, U.K., 1989.

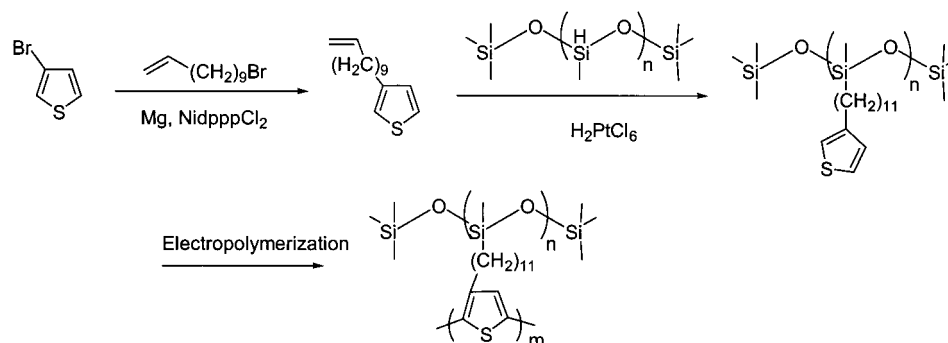
(15) Tamao, K.; Sumitani, K.; Kiso, Y.; Zembayashi, M.; Fujioka, A.; Kodama, S.; Nakajima, I.; Minato, A.; Kumada, M. *Bull. Chem. Soc. Jpn.* **1976**, *49*, 1958.

(16) Han, B. H.; Boudjouk, P. *Organometallics* **1983**, *2*, 769.

(17) Schreiber, R.; Grez, P.; Cury, P.; Veas, C.; Merino, M.; Gómez, H.; Córdova, R.; del Valle, M. A. *J. Electroanal. Chem.* **1997**, *430*, 77.

(18) (a) Ferraris, J. P.; Haillon, T. R. *Polymer* **1989**, *30*, 1319. (b) Yassar, A.; Garnier, F. *Macromolecules* **1989**, *22*, 804. (c) Wei, Y.; Chan, C. C.; Tian, J.; Jang, G. W.; Hseuh, K. F. *Chem. Mater.* **1991**, *3*, 888.

Scheme 2. Synthetic Route for the Monomer and Polymer



diminished. All the films showed a corresponding reduction peak at around 0.55 V. This peak is attributed to the dedoping of the polythiophene.⁹ When the concentration of the precursor polymer is decreased, another peak, ca. 1.06 V, emerges. This new peak is due to the reduction of Au(I) to Au.¹⁹ We have observed this peak in the CV obtained from a plain Au electrode in a polymer-free electrolyte solution. It is quite reasonable that the thinner layers deposited with lower concentrations can cause significant contribution of the Au oxide reduction peak to the CV trace. Nevertheless, this concentration dependence indicates that *cross-linking* is self-limiting especially at lower concentrations as reflected in the CV behavior. *Intermolecular* and *intramolecular* cross-linking is possible although we cannot quantitatively determine the extent of this with current experimental conditions. We can only infer that intermolecular coupling is predominant at higher concentrations based on the probability of chain entanglement²⁰ and concentration of tethered monomer species. Repeated cycling of the electrodeposited polymer film under precursor-polymer-free electrolyte solutions resulted in further current increases. This is another confirmation of the cross-linking mechanism, where kinetically trapped side-group monomer units are able to further cross-link.

It is important to characterize the smoothness of these films, primarily for ultrathin film applications. The film growth and morphology changes were investigated by AFM using the noncontact Mac mode (Figure 2). As previously described, the films were deposited from 0.1 M polymer solutions in methylene chloride with 0.1 M TBAH as supporting electrolyte. A homogeneous and morphologically continuous film was formed on the substrate even after the first cycle. This film is *uniform* throughout the substrate, with very small domain sizes. The AFM images of the films after one to seven cycles all have globular morphologies. As the number of cycles increased, the morphology of the films resulted in increasing domain size up to the first seven cycles. However, there is a significant change in the morphology beginning at the ninth cycle. No regular globular domains were observed from the AFM image similar to the first seven cycles. Instead, these morphologies are diffused and more "membranelike or porous" but still maintained uniformity throughout the film.

This morphological change provides some useful information about the polymer electrodeposition mechanism and film growth. Initially, the nucleation process of electropolymerization for the precursor polymer is fast. When the potential is high enough to oxidize a majority of the thiophene units, coupling occurs and the polymer

becomes insoluble in the solvent (primarily through cross-linking) and immediately deposits on the flat electrode surface.²¹ The uniformity of the film after the first cycle suggests that this fast process is predominant throughout the substrate surface. With the first few cycles, the film grows on these nucleation sites, together with increasing size of the domains and aggregates. We believe that because of the influence of the precursor polymer chain, the morphology is rendered smooth and uniform in contrast to direct electrodeposition of thiophene monomers. As the deposition process slows down and the film grows thicker, the deposition process becomes dominated by mass transport, that is, the ability of electrolyte ions to move between the electrode and solution.⁹ Because the precursor polymer contains an insulating polymer component, this mass transport should decrease as the film becomes thicker. Thus, the peak position is observed to shift at a higher potential. When the film is sufficiently thick to block the electron transfer between the electrode/polymer/solution interface, the cross-linking extent of the outer polymer decreases. This explains the membranelike or diffused morphology observed under AFM, which corresponds to a lower cross-linking extent and hence is dominated by the polymethylsiloxane chains. In addition, after 15 cycles the peak current of the oxidation begins to drop and the film becomes passivating with further potential cycling. The morphology of the film remains the same though.

As has been studied with the electrochemical deposition process of thiophene monomers, both three-dimensional instantaneous (3D) nucleation and two-dimensional instantaneous (2D) nucleation is involved. The contribution of 2D nucleation is important in the first stages of the nucleation process.²² In our case, 2D nucleation governs the early stage, and 3D nucleation then became predominant, as can be clearly seen from the domain size changes in the AFM images. The precursor polymer backbone has an important influence on the deposition process especially at the later stage. For example, an almost layer-by-layer growth (investigated by SPS) is observed in contrast to the direct deposition of monomers. However, for monomer solutions 3D nucleation governs the late stage, which causes rough surface morphology and big aggregates. The mass transfer of the precursor polymer solution to the electrode surface is totally different from that of monomer

(21) Kankare, J. *In Electrical and optical polymer systems - fundamentals, methods, and applications*; Wise, D. L., Wnek, G. E., Trantolo, D. J., Cooper, T. M., Gresser, J. D., Eds.; Marcel Dekker: New York, 1993; p 167.

(22) (a) Hillman, A. R.; Mallen, E. F. *J. Electroanal. Chem.* **1987**, *220*, 351. (b) Li, F.; Albery, W. J. *Electrochim. Acta* **1992**, *37*, 393. (c) Schrebler, R.; Grez, P.; Cury, P.; Veas, C.; Merino, M.; Gomez, H.; Cordova, R.; del Valle, M. A. *J. Electroanal. Chem.* **1997**, *430*, 77.

(19) Wagner, D.; Gerischer, H. *J. Electroanal. Chem.* **1989**, *258*, 127.

(20) Doi, M.; Edwards, S. F. *The Theory of Polymer Dynamics*; Clarendon Press: Oxford, 1986.

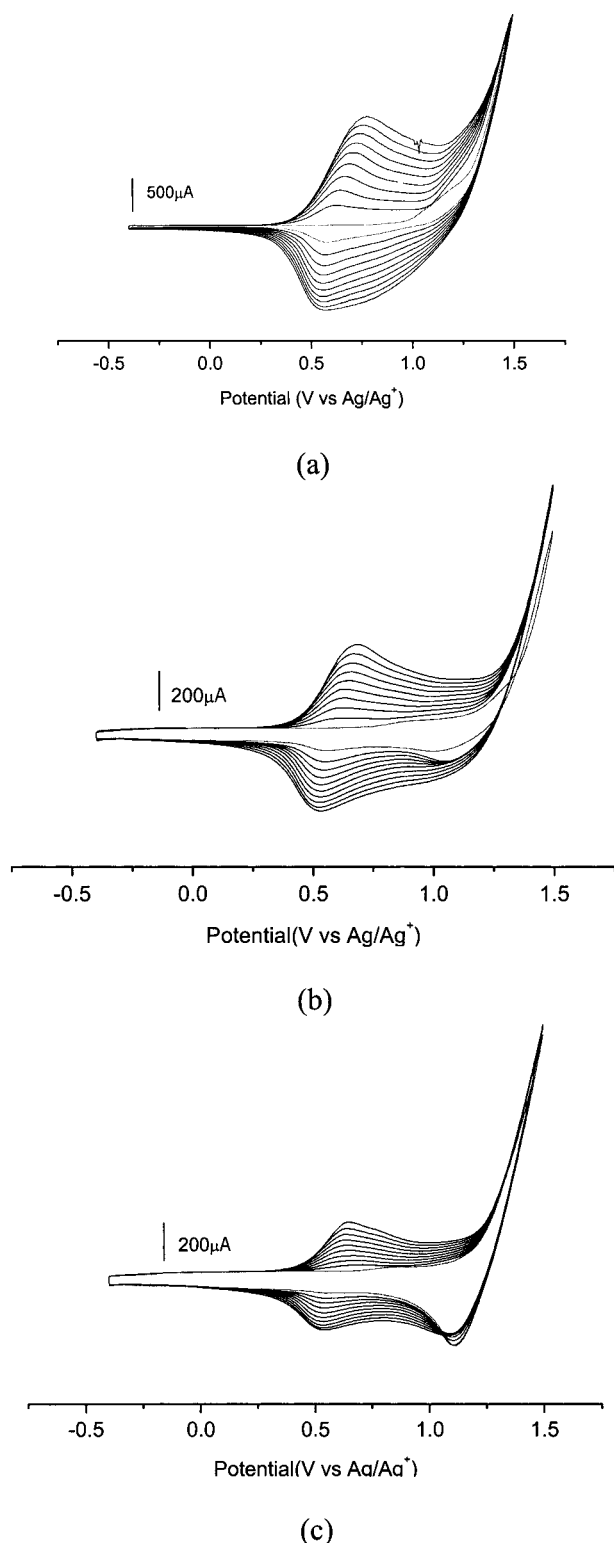


Figure 1. Cyclic voltammogram of the precursor polymer at different concentrations: (a) 0.2 M, (b) 0.1 M, and (c) 0.05 M with 0.1 M TBAAH and methylene chloride. The polymerization was performed by sweeping the potential from -400 to 1500 mV vs the Ag/Ag^+ (0.01 M in ACN) reference electrode.

solutions. This can be further probed by electro-quartz crystal microbalance (EQCM) experiments.²³

To monitor the growth of the films, the films were investigated by SPS.²⁴ Figure 3 shows the increase in

thickness with film growth primarily by the shift in the resonance angle of the plasmon curve. The fact that a plasmon curve was observed is direct evidence of the uniformity and smoothness of the films approaching that of other ultrathin film deposition techniques, for example, Langmuir–Blodgett films, layer-by-layer, spin-coating, and so forth.²⁵ The film has a thickness of ~ 5 nm after the first cycle. The film grows fast initially and becomes easily saturated (nonlinear growth). This phenomenon is consistent with the observation of morphology change and the fact that the electropolymerization ability (extent of cross-linking) changes with thickness. The film has a thickness of ~ 76 nm after 11 cycles. In principle, with the precursor polymer approach, films of various thickness can be easily achieved by controlling the number of cycles. At the same time, the film remains relatively uniform. We are currently investigating the electropolymerization process and the corresponding dielectric constant parameter changes in situ by a simultaneous CV and SPS approach.²⁶

To demonstrate that a polythiophene structure was indeed achieved in the deposited film, the precursor polymer was electrodeposited on a transparent ITO substrate in order to take the transmission UV–vis spectra. The same parameters as for the previous electropolymerization on Au were used. The absorption of the film deposited on ITO from 0.1 M polymer solution in methylene chloride showed a peak at around 440 nm, Figure 4, which is typical for electropolymerized polythiophene films.²⁷ This peak showed a blue shift compared with other substituted polythiophene polymers. This may indicate lower conjugation lengths of the polythiophene structure formed from the precursor polymer than those deposited from monomer solution. This is reasonable since the polymer backbone in the cross-linked system reduces the coupling efficiency compared with the free monomer. Again, the number of electropolymerized thiophene units is not quantifiable on the formed conjugated polythiophene (or even oligothiophene) structures under the current system and experimental setup. Clearly, for electrical conductivity applications a more conjugated system is preferable.¹ The “copolymerization” with free monomers in solution is currently under investigation as well as detailed conductivity experiments. However, for other applications such as hole transport layers for PLED and electrochromic devices, oligomeric thiophene films with high optical quality should be more useful.

XPS measurement of the film (Figure 5) reveals that almost no electrolyte counterions remained in the film after electropolymerization, washing, and drying. No detectable signal from the fluorine component of tetrabutylammonium hexafluorophosphate was observed. This indicates that after holding the potential at the initial potential (last step of the potential cycling) and thoroughly washing with various solvents, the film was totally dedoped and all the counterions were excluded from the film. The peaks from C, O, and Si can be clearly seen from the spectrum. Due to the low sensitivity to XPS and relatively low content, the S peak is not obvious.

Conclusions

A precursor polymer approach to electrodeposition of ultrathin films of conjugated polymers has been demon-

(25) Ulman, A. *An Introduction to Ultrathin Organic Films. From Langmuir–Blodgett to Self-Assembly*; Academic Press: Boston, 1991.

(26) Baba, A.; Advincula, R.; Knoll, W. *Polym. Mater. Sci. Eng. Prepr.* **2001**, *85*, 21.

(27) Zotti, G.; Zecchin, S.; Berlin, A.; Schiavon, G.; Giro, G. *Chem. Mater.* **2001**, *13*, 43.

(23) Mo, Y.; Euijin, H.; Scherson, D. *Anal. Chem.* **1995**, *67*, 2415.

(24) Knoll, W. *Annu. Rev. Phys. Chem.* **1998**, *49*, 569.

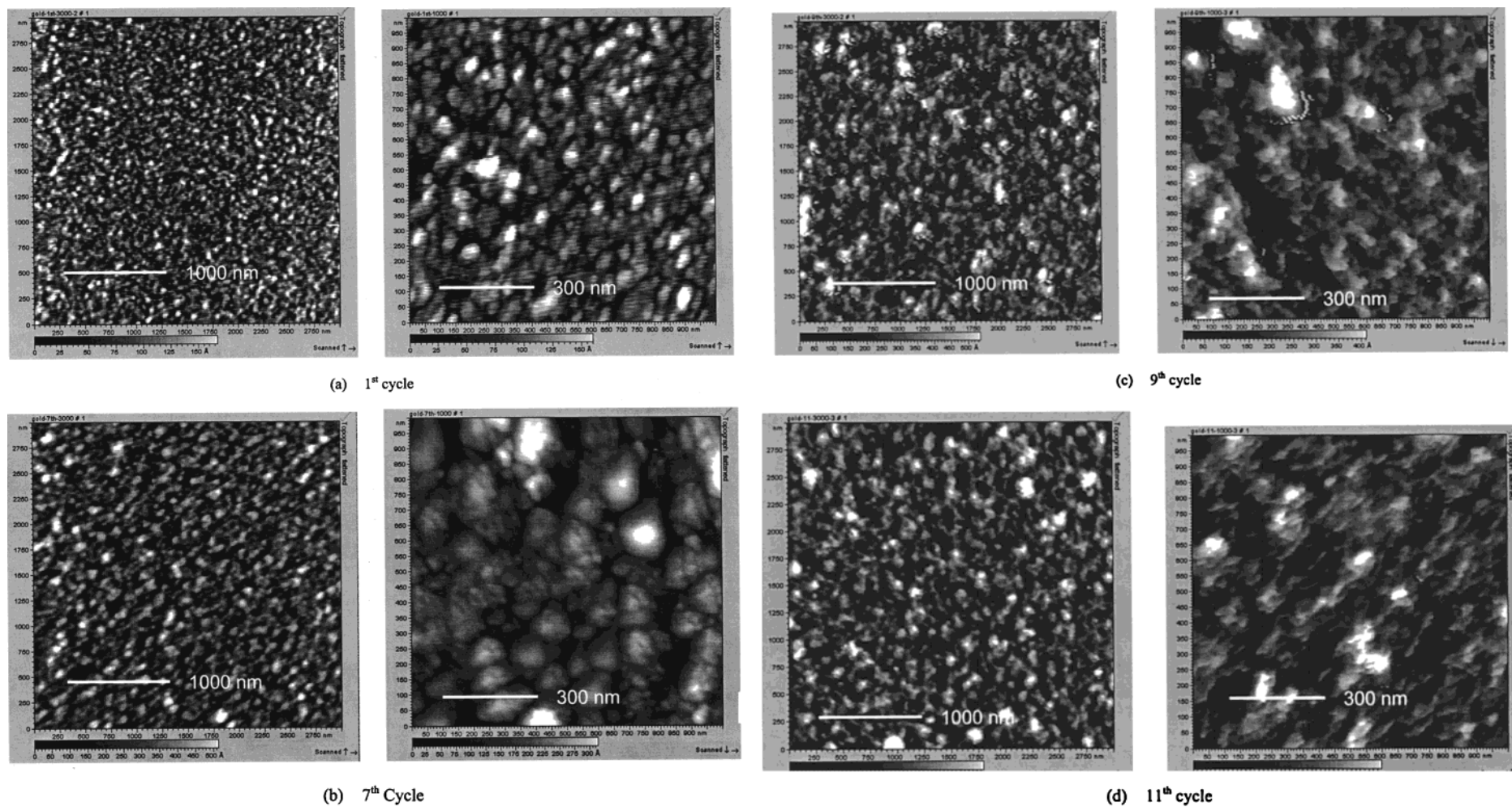


Figure 2. AFM of the growth of the precursor polymer film on gold at different potential cyclings. Imaging was performed in air at ambient temperature using Mac mode.

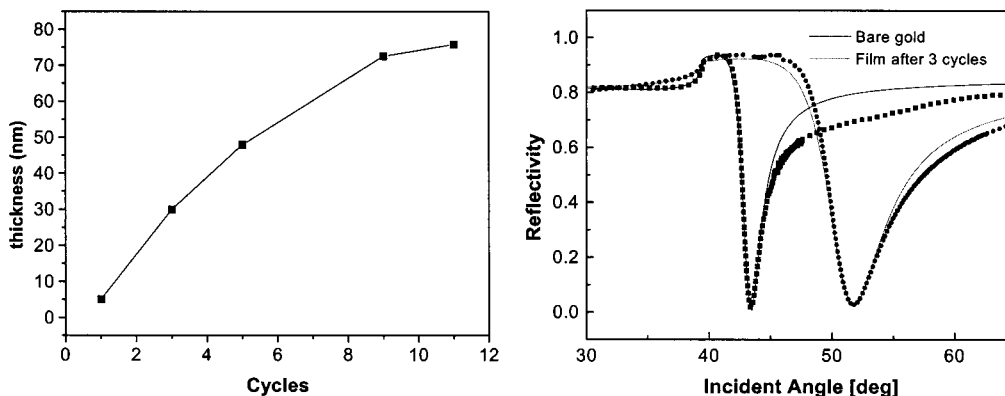


Figure 3. Thickness study by SPS showing a layer-by-layer growth with each deposition.

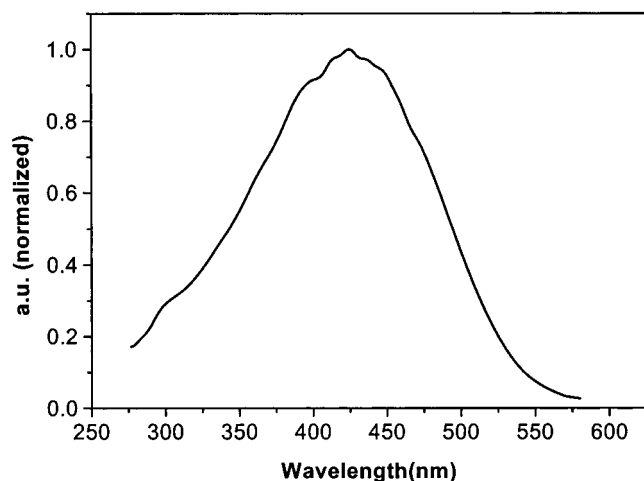


Figure 4. UV-vis spectrum of the electrodeposited film on ITO using the same conditions as with the Au electrode.

strated with polythiophene. The precursor polymer contains a polysiloxane backbone with pendant thiophene units as the electroactive group. The thiophene units polymerized upon sweeping the potential at the proper range. A uniform and smooth film morphology was observed. The cyclic voltammogram and UV-vis spectra showed clear evidence of polythiophene structure in the cross-linked polymer. The morphology of the film as probed by AFM changed with increasing number of cycles. It transformed from a relatively globular morphology to a more membranelike one, which is consistent with the electropolymerization process and extent of cross-linking. The polymethylsiloxane backbone plays an important role in determining the film morphology especially at thicker

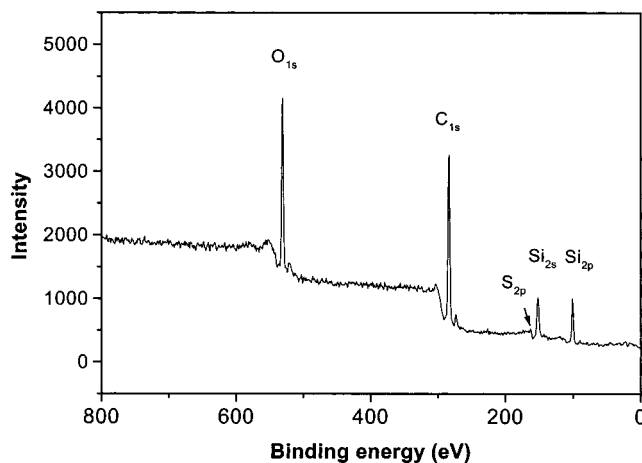


Figure 5. XPS of the electrodeposited polymer film on Au was done from 0 to 1400 eV.

deposited films. Film thickness was monitored by surface plasmon spectroscopy, with the thickness of the deposited polymer film easily controlled by the number of cycles.

Acknowledgment. We gratefully acknowledge partial funding from the NSF CAREER Award (DMR 99-82010) and helpful discussions with Akira Baba, Wolfgang Knoll, Daniel Roitman, and Seiji Inaoka. We also acknowledge Molecular Imaging, Inc. and Dr. Earl Ada (UA Tuscaloosa) for technical support.

LA011259D